A Shape Memory Acrylamide/DNA Hydrogel Exhibiting Switchable Dual pH-Responsiveness

*Yuwei Hu, Chun-Hua Lu, Weiwei Guo, Miguel Angel Aleman-Garcia, Jiangtao Ren, and Itamar Willner**

Shape memory acrylamide/DNA hydrogels include two different crosslinkers as stabilizing elements. The triggered dissociation of one of the crosslinking elements transforms the shaped hydrogel into an arbitrarily shaped (or shapeless) quasi-liquid state. The remaining crosslinking element, present in the quasi-liquid, provides an internal memory that restores the original shaped hydrogel upon the stimulus-triggered regeneration of the second crosslinking element. Two pH-sensitive shape memory hydrogels, forming Hoogsten-type triplex DNA structures, are described. In one system, the shaped hydrogel is stabilized at pH = 7.0 by two different duplex crosslinkers, and the transition of the hydrogel into the shapeless quasi-liquid proceeds at pH = 5.0 by separating one of the crosslinking units into a protonated cytosine–guanine–cytosine (C–G·C$^+$) triplex. The second shaped hydrogel is stabilized at pH = 7.0, by cooperative duplex and thymine–adenine–thymine triplex (T–A·T) bridges. At pH = 10.0, the triplex units separate, leading to the dissociation of the hydrogel into the quasi-liquid state. The cyclic, pH-stimulated transitions of the two systems between shaped hydrogels and shapeless states are demonstrated. Integrating the two hydrogels into a shaped "two-arrowhead" hybrid structure allows the pH-stimulated cyclic transitions of addressable domains of the hybrid between shaped and quasi-liquid states.

1. Introduction

Shape memory polymers represent an interesting class of materials that are processed into a permanent shaped structure that undergoes a stimuli-triggered transition into a temporary arbitrarily shaped or shapeless structure that includes an internal memory to regenerate, in the presence of an appropriate stimulus, the original shape.[1] Different applications of shape memory hydrogels were suggested, and these include sensing,[2] operation as valves or actuators,[3] controlled drug delivery,[4] and inscription of information.[5] Also, hydrogels with dual shape memory properties were reported.[6] The base sequence in nucleic acids provides a means to encode information into the biopolymer that allows the stimuli-triggered reversible transitions of the nucleic acids between two states.[7] Different stimuli, such as pH,[8] metal-ion/ligand,[9] or photonic signal,[10] were applied to switch DNA structures such as duplex DNAs, i-motif, or G-quadruplex structures, and these triggering signals were used to design DNA switches or DNA devices in solutions[11] and on surfaces.[12] DNA-based hydrogels attract recent research efforts, and stimuli-responsive hydrogels undergoing switchable hydrogel/solution transitions were developed.[13] pH-responsive hydrogels composed of i-motif[13g] or nucleic acid triplex bridges,[14] metal-ion-assisted cooperative bridging of duplex nucleic acids[15] or K$^+$-ion-stabilized G-quadruplex bridges,[13b] and their dissociation in the presence of ligands or receptors were applied to reversibly switch hydrogels-to-solution transitions. Different applications of stimuli-responsive hydrogels were suggested, including controlled drug release,[16] sensors,[17] switchable catalysis,[13b] tailoring of separation matrices,[18] and the activation of enzyme cascades.[19] Recently, a pH-responsive shape memory acrylamide DNA-hydrogel was reported.[13g,20] In this system, the shaped hydrogel was stabilized by bridging the acrylamide chains with two types of cooperative crosslinking elements involving duplex DNA and pH-sensitive i-motif units. The pH-stimulated separation of the i-motif dissociated the hydrogel into a quasi-liquid state, where the entanglement of the polymer chains by the residual duplex units provided a temporary memory for restoring the original shape upon reforming the i-motif bridging units. The development of other shape memory hydrogels, and particularly, the conjugation of hybrid shape memory polymers triggered by different stimuli, remains a challenge in materials science. Here we wish to report on the preparation of different pH-responsive shape memory hydrogels composed of acrylamide chains crosslinked by duplex DNA and pH-sensitive triplex DNA crosslinking units. In contrast to the previously reported system, the shape memory hydrogels exist at neutral pH as stable hydrogels, and are dissociated to quasi-liquid states either at acidic pH values (pH = 5.0) or at basic pH values (pH = 10.0). We further demonstrate the integration of two pH-sensitive hydrogels into a hybrid two-domain shaped structure, where each domain can be selectively addressed to undergo hydrogel/quasi-liquid shape memory dictated transitions.

Dr. Y. Hu, Dr. C.-H. Lu, Dr. W. Guo,
Dr. M. A. Aleman-Garcia, Dr. J. Ren, Prof. I. Willner
Institute of Chemistry and the Center for Nanoscience and Nanotechnology
The Hebrew University of Jerusalem
Jerusalem 91904, Israel
E-mail: willnea@vms.huji.ac.il

DOI: 10.1002/adfm.201503134

© 2015 WILEY-VCH Verlag GmbH & Co. KGaA, Weinheim

The stabilization of pH-induced Hoogsteen-type triplex DNA structures is well established,[14] and the pH-stimulated cyclic transitions between triplex and duplex structures were used to operate different DNA switches.[21] The cooperative stabilization of protonated C–G·C$^+$ triplex bridges at pH = 5.0 transforms duplex structures at neutral pH to triplex configuration at acidic pH values. Alternatively, triplex T–A·T bridges are stabilized at neutral pH, and these dissociate at pH = 10.0 to duplex T–A structures, due to the deprotonation of the thymine residues. These two types of Hoogsteen interactions stabilizing triplex structures were applied to prepare shape-memory hydrogels.

2. Results and Discussion

Figure 1A depicts the synthesis and shape memory properties of the C–G·C$^+$-stabilized hydrogel. Three different acrydite nucleic acid monomers (**1**), (**2**), (**3**), and acrylamide, at a ratio of 5:5:4:700, are used to generate the polymer. The molecular weight of the polymer was estimated to be ≈160 000, using Nuclear Magnetic Resonance (NMR) spectroscopy[14] (Figure S1, Supporting Information), and the ratio of DNA subunits to unsubstituted acrylamide units was determined spectroscopically to be 1:50 (Figure S2, Supporting Information). The acrydite nucleic acid (**1**) includes the base sequence capable of forming the triplex structure at pH = 5.0. At pH = 7.0 the tether I being a part of (**1**) exists in a free, flexible, configuration, and the domain II exists as an intramolecular stabilized duplex. The tether I is complementary to the nucleic acid associated with (**2**), and forms a duplex structure with the free tether I at neutral pH. At pH = 5.0 the intramolecular triplex structure between subunits I and II of (**1**) is energetically stabilized. The nucleic acids associated with (**3**) are self-complementary and exist in a (**3**)/(**3**) duplex structure at pH = 7.0 and pH = 5.0. The preparation of the shaped hydrogel and its operation as a shape memory hydrogel are presented in Figure 1A. The as-prepared acrylamide/(**1**)-, (**2**)-, (**3**)-acrylamide chains in a pH = 7.0 buffer were heated to form a solution, and

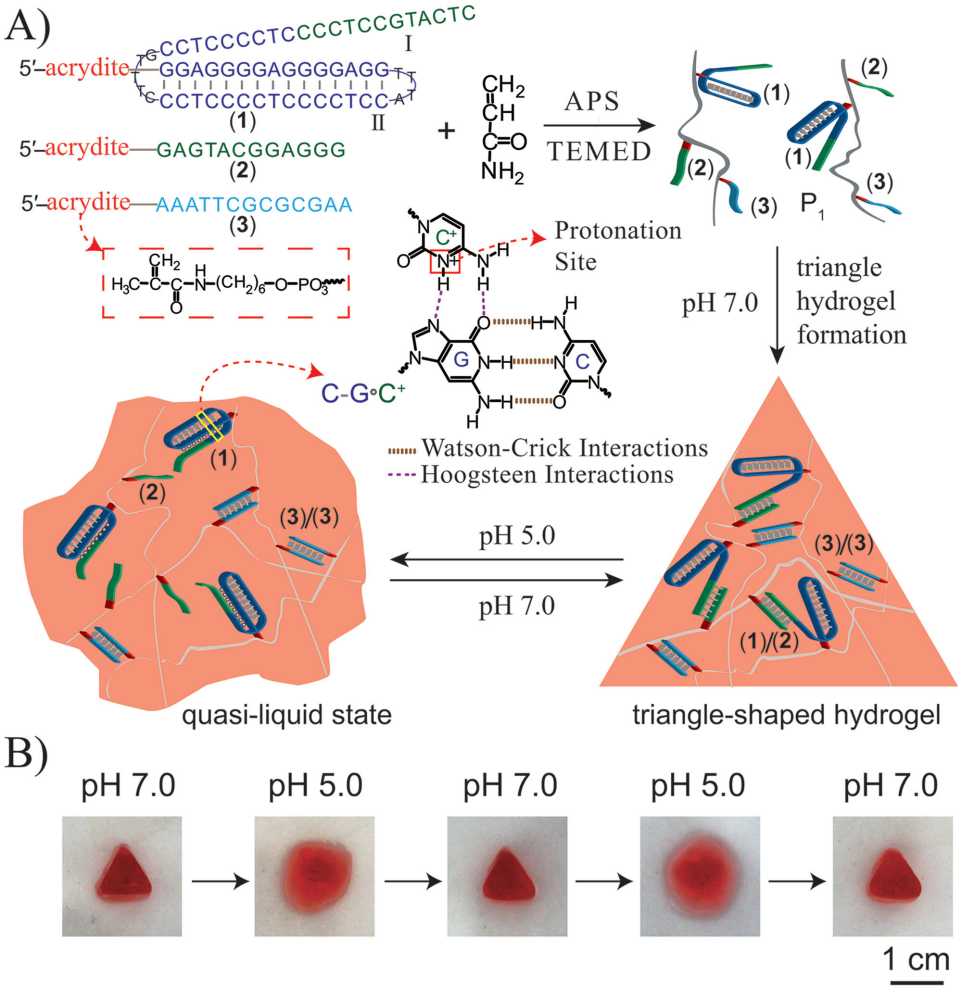

Figure 1. A) Schematic synthesis and switchable pH-stimulated hydrogel/quasi-liquid transitions of a shape memory hydrogel composed of a duplex nucleic acid (permanent memory) and C–G·C$^+$ triplex crosslinking units. B) Images corresponding to the cyclic pH-stimulated transitions of a shaped (triangle) hydrogel and a shapeless quasi-liquid state upon the reversible subjecting of the system to pH = 7.0 and pH = 5.0, respectively. (The hydrogel is stained with Gel Red.) Experiments were conducted at 25 °C. The transitions shown in (B) could be cycled for at least five times, without affecting the shape memory properties of the hydrogels.

© 2015 WILEY-VCH Verlag GmbH & Co. KGaA, Weinheim

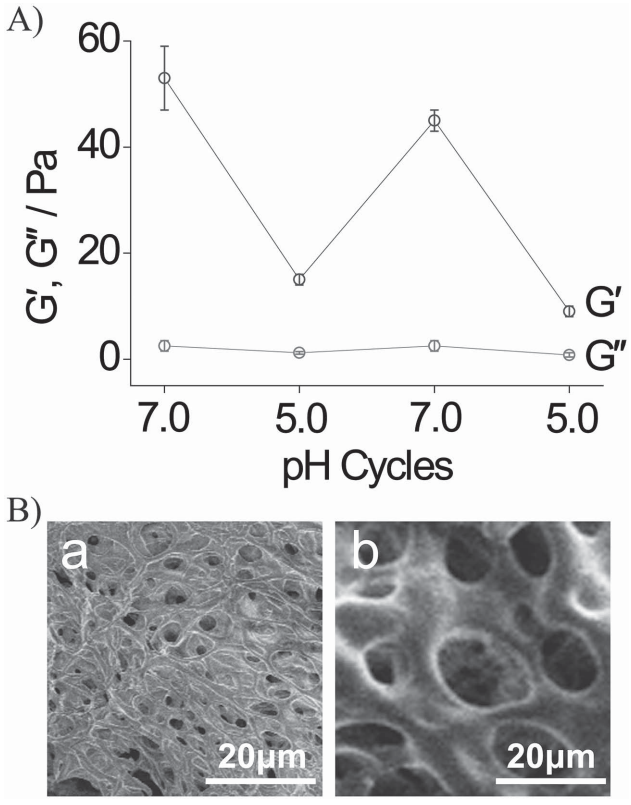

Figure 2. A) Rheometric characterization of the pH-stimulated transitions between the (**1**)/(**2**) and (**3**)/(**3**)-crosslinked hydrogel and the quasi-liquid state crosslinked by the (**3**)/(**3**) duplexes: G′-values of the storage modulus, G″-values of the loss modulus. Error bars derived from $N = 3$ measurements. B) SEM images of the: a) the freeze-dried, Au/Pd-coated, (**1**)/(**2**) and (**3**)/(**3**)-crosslinked hydrogel; b) the freeze-dried, Au/Pd-coated, (**3**)/(**3**)-crosslinked quasi-liquid system. Experiments were conducted at 25 °C.

that was introduced into a triangle-shaped mold. Upon cooling, the hydrogel stabilized by cooperative duplexes between domain I of (**1**) and (**2**) and (**3**)/(**3**) was formed. The triangle-shaped hydrogel was extracted from the mold. Subjecting the hydrogel to pH = 5.0 dissociated the (**1**)/(**2**) duplexes, due to the stabilization of the (**1**)-triplex state. The elimination of the (**1**)/(**2**) duplex crosslinking units results in the dissociation of the hydrogel into a shapeless quasi-liquid phase. The residual duplex crosslinking units (**3**)/(**3**) provide, however, a dictated spatial structural entanglement of the polymer chains that provide an internal memory in the polymer network to reshape the hydrogel. Subjecting the quasi-liquid state to pH = 7.0 dissociates the triplex units, resulting in the network-dictation hybridization of the (**1**)/(**2**) duplex units and the reshaping of the hydrogel. Figure 1B depicts the cyclic pH-stimulated transitions between the triangle-shaped hydrogel (pH = 7.0) and the quasi-liquid shapeless droplet (pH = 5.0). Rheometry experiments, **Figure 2**A, and metal-coated Scanning Electron Microscopy (SEM) images, Figure 2B, confirmed the hydrogel/quasi-liquid transitions. The hydrogel at pH = 7.0 shows a high storage modulus, G′, of ≈50 Pa, whereas the quasi-liquid system exhibits a low storage modulus, G′, of ≈15–18 Pa. The loss modulus of the two systems is ≈2 Pa. The SEM image of the hydrogel (pH = 7.0) shows a rough porous structure, while the quasi-liquid system shows a smooth structure (Figure 2B(a) and (b), respectively). The porosity of the hydrogel as well as its storage modulus G′ is controlled by the degree of the crosslinking of the hydrogel by means of the two crosslinking motives. Reducing the loading of the crosslinking motives increases the porosity of the hydrogel, while increasing the degree of crosslinking decreases the porosity. The different porosities affect the shape memory properties of the resulting hydrogel. While lower crosslinking perturbs the quality of the resulting hydrogel shape, lower porosity introduces barriers to dissociate the shaped structures. The results represent the optimized loading of the polymer chain to yield the shape-memory properties. It should be noted that the shape memory properties of the hydrogel can be measured up to 40 °C.

The second triplex DNA-based shaped hydrogel is depicted in **Figure 3**A. The hydrogel was synthesized by the radical-induced polymerization of the acrydite nucleic acid (**3**), the acrydite nucleic acids (**4**), and acrylamide at a molar ratio corresponding to 4:9:260. The molecular weight of the resulting polymer corresponded to 180 000 and the ratio of loaded nucleic acids:acrylamide units corresponded to 1:20 (Figure S3, Supporting Information).

The resulting polymer chains exhibit self-complementarity of the tethers (**3**)/(**3**), leading to insufficient crosslinking stabilization to form a hydrogel. The polymer solution was introduced into the triangle-shaped mold, and in the presence of the added strand (**5**), the hydrogel was formed in the mold. The hydrogel at pH = 7.0 is stabilized by the (**3**)/(**3**) duplex bridges and by Hoogsteen-type triplex T–A·T-based crosslinking units composed of (**4**)/(**5**)/(**4**). The shaped hydrogel excluded from the mold was subjected to pH = 10.0 that separated the triplex DNA bridges. This resulted in the separation of the hydrogel into a quasi-liquid state, where the residual duplex units bridging the entangled polymer network provide the permanent memory for regeneration of the hydrogel shape. Subjecting the quasi-liquid, shapeless, polymer solution to pH = 7.0 regenerates the cooperative stabilizing crosslinking interactions composed of the duplexes (**3**)/(**3**) and the triplex units (**4**)/(**5**)/(**4**), resulting in the triangle-shaped hydrogel. By the cyclic treatment of the system at pH = 7.0 and pH = 10.0 the system could be switched between the shaped and quasi-liquid states (Figure 3B). **Figure 4**A depicts the switchable rheometric properties of the system. While the hydrogel consisting of cooperatively stabilized crosslinked network composed of the (**3**)/(**3**) and triplex (**4**)/(**5**)/(**4**) bridges reveals a high storage modulus, G′ = 70 Pa, the quasi-liquid shows a very low storage modulus, G′, ≈20 Pa (Figure 4A). The SEM images of the metal-coated hydrogel and quasi-liquid systems (Figure 4B) further support the pH-stimulated phase transitions of the systems. While the hydrogel formed at pH = 7.0 reveals a highly porous network of the hydrogel, panel (a), the quasi-liquid state shows a fluidic, substantially smoother structure, panel (b).

Finally, the two pH-sensitive, shape memory, hydrogels were integrated into one hybrid structure that undergoes programmed shape memory transitions upon subjecting the structure to three different pH values: 5.0, 7.0, and 10.0. The construction of the hybrid pH-sensitive shape memory

© 2015 WILEY-VCH Verlag GmbH & Co. KGaA, Weinheim

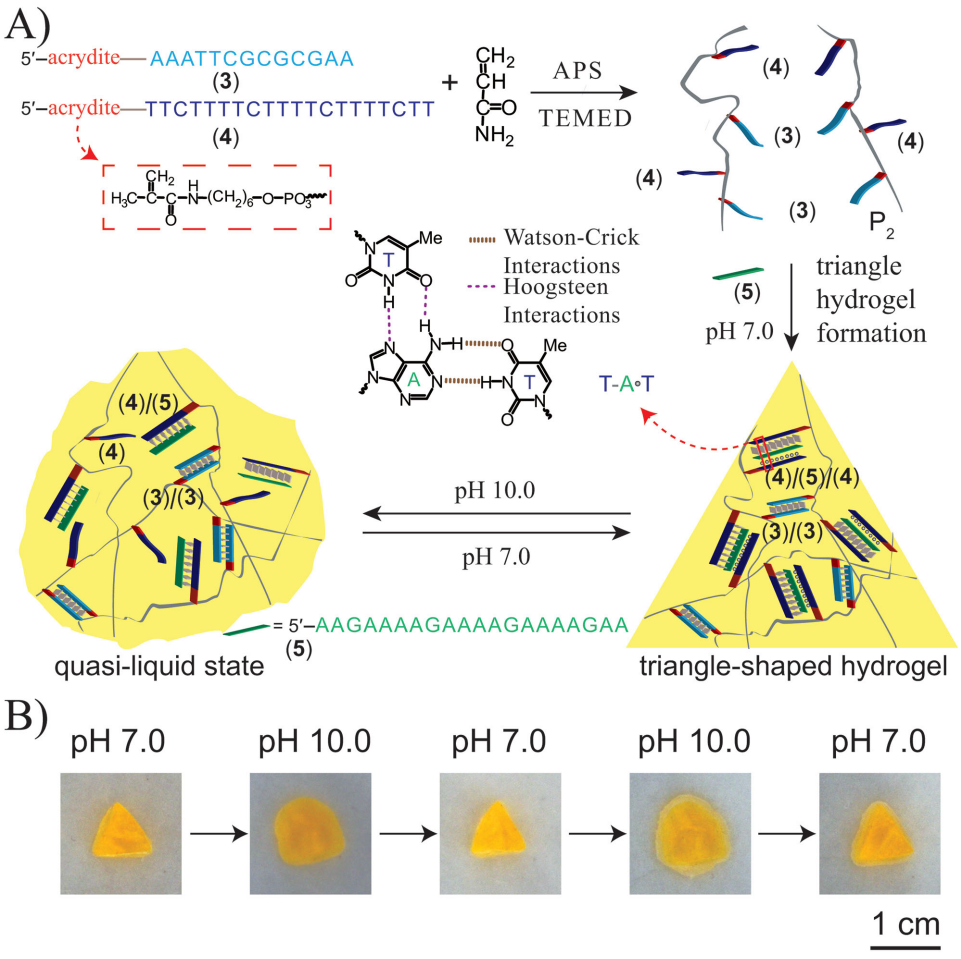

Figure 3. A) Schematic synthetic and switchable pH-stimulated hydrogel/quasi-liquid transitions of a shape memory hydrogel composed of a duplex nucleic acid (permanent memory) and T–A·T triplex crosslinked units. B) Images corresponding to the cyclic pH-stimulated transitions of a shaped (triangle) hydrogel and a shapeless quasi-liquid state upon the reversible subjecting of the system to pH = 7.0 and pH = 10.0, respectively. (The hydrogel is stained with SYBR Green I). Experiments were conducted at 25 °C. The transitions shown in (B) can be cycled for at least five times, without affecting the shape memory properties of the hydrogels.

hydrogel structure and its operation are depicted in **Figure 5**. The polymer chains shown in Figures 1A and 3A were synthesized in the presence of the acrydite nucleic acid L and L′, respectively, where L and L′ are complementary—that is the pH 7.0/5.0 shape memory hydrogel includes the L tethers and the pH 7.0/10.0 shape-memory hydrogel includes the L′ as additional functionality. The hybridization between L/L′ provides the principle to integrate the two hydrogels into the hybrid structure. This is presented in Figure 5A with the assembly of the integrated hybrid hydrogel consisting of a two-arrowhead structure. The mold includes the two arrowhead shapes as shown in Figure 5B. The blocker unit (blue) was placed in the mold, and the liquefied polymer mixture consisting of the acrylamide chains modified by (**1**), (**2**), (**3**), and L (ratio (**1**):(**2**):(**3**):L was 5:5:4:4) were introduced into the left compartment of the mold and allowed to gelate at pH = 7.0. The dye, Gel Red (red), was incorporated into the hydrogel to allow the imaging of the structure. After the hydrogelation was completed, the blocker unit was removed from the mold, and the hot solution of the polymer chains composed of the acrylamide and the nucleic acid tethers (**3**), (**4**), (**5**), and L′ (ratio (**3**):(**4**):(**5**):L′ was 4:9:4.5:4) were added to the right compartment of the mold, and the solution was allowed to cool down and hydrogelate. The dye, SYBR Green | (yellow), was incorporated in the polymer solution and in the resulting hydrogel for imaging purposes. The hybrid two-component hydrogel was then removed from the mold to yield the two-arrowhead structure. It should be noted that heating of the polymer solution introduced into the right compartment was essential to yield the stable interlinked hybrid structure of the two polymers. Presumably, the local heating of the boundary between the two polymers liquefies the boundary region, thus allowing enhanced hybridization between the interlinking tethers L/L′. Figure 5C depicts the programmed dual pH-stimulated structural transitions of the two shape memory hydrogels. Subjecting the two-arrowhead structure to pH = 5.0 transforms the hydrogel "A" (red) into a quasi-liquid state, while the hydrogel "'B" (yellow) retains its original structure. Treatment of the system at pH = 7.0 restores the original two-arrowhead structure, consistent with the shape memory properties of the quasi-liquid system "A." Further reaction of

© 2015 WILEY-VCH Verlag GmbH & Co. KGaA, Weinheim

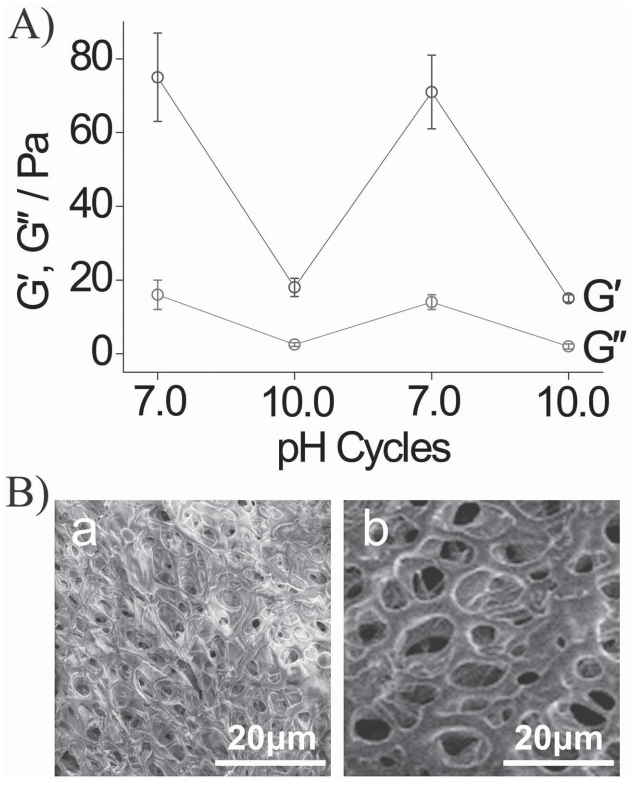

Figure 4. A) Rheometric characterization of the pH-stimulated transitions between the (**4**)/(**5**)/(**4**) and (**3**)/(**3**)-crosslinked hydrogel and the quasi-liquid state crosslinked by the (**3**)/(**3**) duplexes: G′-values of the storage modulus, G″-values of the loss modulus. Error bars derived from $N = 3$ measurements. B) SEM images of the: a) the freeze-dried, Au/Pd-coated, (**4**)/(**5**)/(**4**) and (**3**)/(**3**)-crosslinked hydrogel; b) the freeze-dried, Au/Pd-coated, (**3**)/(**3**)-crosslinked quasi-liquid system. Experiments were conducted at 25 °C.

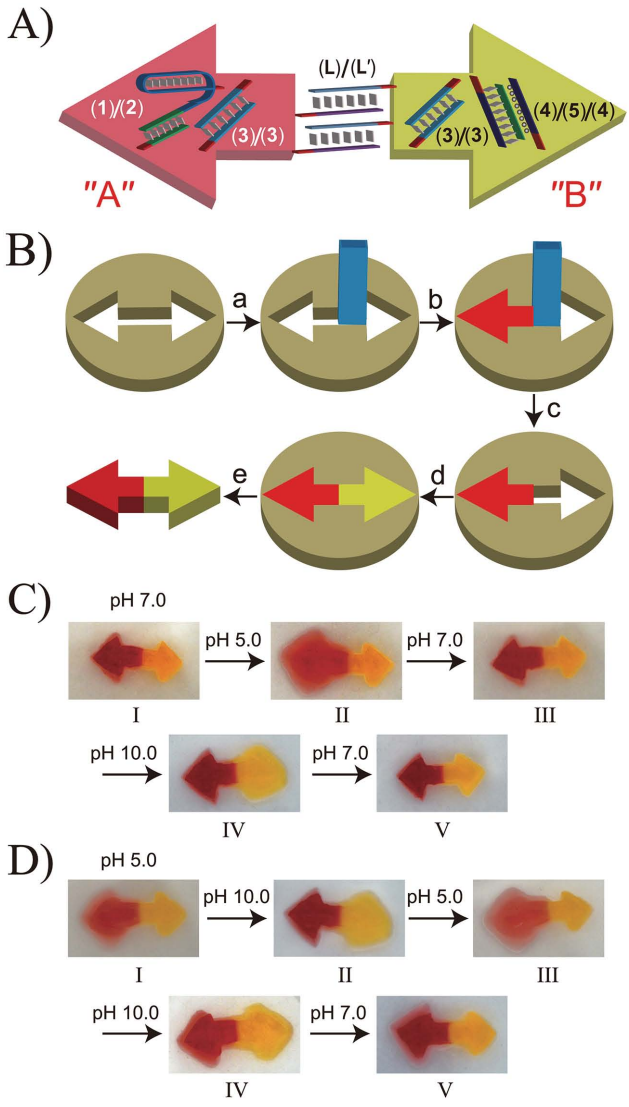

Figure 5. A) Schematic hybrid "two-arrowhead" two-hydrogel structure composed of a (**1**)/(**2**) and (**3**)/(**3**)-crosslinked hydrogel, undergoing hydrogel/quasi-liquid transitions at pH = 7.0 and 5.0, respectively, and a (**4**)/(**5**)/(**4**) and (**3**)/(**3**)-crosslinked hydrogel, undergoing hydrogel/quasi-liquid transitions at pH = 7.0 and 10.0, respectively. B) Formation of the hybrid hydrogel in the mold, and extraction of the two-arrowhead-shaped structure: a) blocking the two-arrowhead mold with a blocker unit (blue); b) assembly of the (**1**)/(**2**) and (**3**)/(**3**)-crosslinked hydrogel arrowhead domain, "A" (red); c) removal of the blocker unit; d) growing the (**4**)/(**5**)/(**4**) and (**3**)/(**3**)-crosslinked hydrogel, "B" (yellow), in the vacant reservoir; e) removal of the hybrid hydrogel from the mold. C) Cyclic pH-triggered transitions of the hybrid two-arrowhead structure (pH = 7.0, I) upon its subjection to a pH cycle 5.0 (II)→ 7.0 (III)→ 10.0 (IV)→ 7.0 (V). D) Cyclic pH-triggered transitions of the hybrid two-arrowhead structure upon subjecting the system to a pH cycle corresponding to 5.0 (I)→ 10.0 (II)→ 5.0 (III)→ 10.0 (IV)→ 7.0 (V). Experiments were conducted at 25 °C.

the resulting system at pH = 10.0 transforms hydrogel "B" into a quasi-liquid state that exhibits shape memory properties, and upon treatment at pH = 7.0, restores the original shape of the hybrid two arrowheads. Also, the treatment of the system comprising the shapeless quasi-liquid phase of "A" and the intact hydrogel "B" at pH = 10.0 restores the structured hydrogel "A", while transforming the hydrogel "B" into the quasi-liquid phase (Figure 5D). The further treatment of the resulting system at pH = 5.0 restores the structure of the hydrogel "B", while transforming the hydrogel "A" into the quasi-liquid state. Any of the systems, which include one of the hydrogel domains in a quasi-liquid state, at pH = 7.0, restores the intact two-arrowhead structure of the two hydrogels.

3. Conclusions

In conclusion, the present study has tailored acrylamide/DNA hydrogels based on, Hoongstean-type, triplex DNA units that exhibit pH-responsiveness and shape memory properties. The important novel features of the systems include: i) We designed two systems that exist as hydrogels at pH = 7.0. One of the systems is transformed at pH = 5.0 to the quasi-liquid state, while the other hydrogel is transformed at pH = 10.0 into the quasi-liquid state. ii) The two hydrogels exhibit shape memory properties due to the crosslinking of the hydrogels by two cooperative crosslinking elements. The two cooperatively operating crosslinking elements stabilize the hydrogel structures, whereas the pH-triggered dissociation of one of the

© 2015 WILEY-VCH Verlag GmbH & Co. KGaA, Weinheim

crosslinking elements dissolves the hydrogels into quasi-liquid, shapeless states. The residual duplex nucleic acids, present in the quasi-liquids, provide an internal "memory" to reshape the hydrogel structures. iii) A hybrid structure of the two pH-responsive, shape memory hydrogels was constructed. The programmed pH-triggered transitions of the hydrogel domains of the hybrid between shaped and quasi-liquid configurations was demonstrated.

4. Experimental Section

Materials: HEPES sodium salt, magnesium chloride, ammonium persulfate (APS), N,N,N′,N′-Tetramethylethylenediamine (TEMED), and acrylamide solution (40%) were purchased from Sigma-Aldrich. SYBR Green I was purchased from Life Technologies Corporation (USA). Gel Red was purchased from Biotium, Inc., USA. Desalted 5′ end acrydite-modified nucleic acid strands were purchased from Integrated DNA Technologies Inc. (Coralville, IA). Ultrapure water purified by a NANOpure Diamond instrument (Barnstead International, Dubuque, IA, USA) was used to prepare all of the solutions. The sequences used in the study are the following:

(1) 5′-acrydite-GGA GGG GAG GGG AGG TTT ACC TCC CCT CCC CTC CCT TTG CCT CCC CTC CCC TCC GTA CTC-3′
(2) 5′-acrydite-GAG TAC GGA GGG-3′
(3) 5′-acrydite-AAA TTC GCG CGA A-3′
(4) 5′-acrydite-TTC TTT TCT TTT CTT TTC TT-3′
(5) 5′-AAG AAA AGA AAA GAA AAG AA-3′

(**L**) 5′-acrydite-CCT TAT CAT ATC TCT AGA CTA TCA-3′

(**L′**) 5′-acrydite-GTT GAT AGT CTA GAG ATA TGA TAA-3′

Synthesis of the Acrylamide/Acrydite-Nucleic Acid Copolymers: The system shown in Figure 1A consisting of the (**1**)/(**2**) and (**3**)/(**3**) crosslinked hydrogel was prepared as follows: A buffer solution (HEPES, 10×10^{-3} M, $MgCl_2$, 100×10^{-3} M, pH = 7.0), 150 µL, which included 2% acrylamide and the acrydite-modified DNA strands (**1**), 0.5×10^{-3} M, (**2**), 0.5×10^{-3} M, and (**3**), 0.4×10^{-3} M, was prepared. Nitrogen was bubbled through the solution. Subsequently, 10 µL of a 0.2 mL aqueous solution that included 20 mg APS and 10 µL TEMED was added to the mixture of monomers. The resulting solution was allowed to polymerize at room temperature for 5 min, and then the solution was further polymerized at 4 °C for 12 h. The resulting copolymer was purified from unreacted monomer units, salts, and the initiators, using a Microcon (Millipore) spin filter unit (MWCO 10 kD). The purified polymer was removed from the filter and dried under a gentle nitrogen flow. The concentrations of the copolymer chains and the ratio of the acrylamide/acrydite-nucleic acid units were determined spectroscopically (see Figure S2, Supporting Information).

For the preparation of the hydrogel shown in Figure 3A, an acrylamide copolymer chain composed of acrylamide/acrylamide (**3**)/and acrylamide (**4**) monomer units was prepared. A buffer solution (HEPES, 10×10^{-3} M, $MgCl_2$, 100×10^{-3} M, pH = 7.0), 150 µL, which included 2% acrylamide, the acrydite-modified DNA strand (**3**), 0.4×10^{-3} M, and the acrydite-modified DNA strand (**4**), 0.9×10^{-3} M, was prepared. 10 µL of a 0.2 mL aqueous solution that included APS, 20 mg, and TEMED, 10 µL, was added to the mixture. The resulting solution was allowed to polymerize at room temperature for 5 min and then the solution was further polymerized at 4 °C for 12 h. The resulting co-polymer was purified from unreacted monomer units, salts, and initiators, using a Microcon (Millipore) spin filter unit (MWCO 10 kD). The purified polymer was removed from the filter and dried under a gentle nitrogen flow. The concentrations of the copolymer chains and the ratio of the acrylamide/acrydite-nucleic acid units were determined spectroscopically (see Figure S3, Supporting Information). To the aqueous solution, HEPES buffer solution, pH = 7.0, that included the polymer chain acrylamide/(**3**)/(**4**), 150 µL, the strand (**5**), 0.4×10^{-3} M, was added to form the hydrogel.

Determination of the Ratio of Acrylamide/Acrydite-Nucleic Acid Units in Copolymer Chains: To a solution containing the respective acrydite nucleic acids, 0.5×10^{-6} M, variable concentrations of the pure acrylamide polymer were added, and the absorption spectra of the different solutions were recorded. The increase in the absorbance at $\lambda = 200$ nm corresponded to the nonsubstituted polyacrylamide chains, while the absorbance at around $\lambda = 260$ nm corresponded to the acrydite-nucleic acid units. An appropriate calibration curve corresponding to the molar ratio of the nucleic acids in the copolymer and the acrylamide monomer units was derived. Based on this calibration curve, the ratio of acrydite-nucleic acid/acrylamide in the different copolymers was evaluated spectroscopically (for the copolymer shown in Figure 1A, see Figure S2, Supporting Information; for the copolymer system shown in Figure 2A, see Figure S3, Supporting Information).

Preparation of a Triangle-Shaped Hydrogel and the pH- Triggered Transitions between Hydrogel and Quasi-liquid States: To form a triangle-shaped (**1**)/(**2**) and (**3**)/(**3**) crosslinked hydrogel, the dried copolymer sample was dissolved in a 150 µL HEPES buffer (10×10^{-3} M HEPES, 100×10^{-3} M $MgCl_2$, pH 7.0) to yield a mixture containing 1.08×10^{-3} M nucleic acids. The resulting mixture was heated to 95 °C, to yield a homogenous aqueous polymer solution. The hot solution was poured into a triangle-shaped tetrafluoroethylene mold, and was allowed to cool down to room temperature. After incubation for 2 h, the resulting shaped (**1**)/(**2**) and (**3**)/(**3**) crosslinked hydrogel was removed from the mold.

To form a triangle-shaped (**4**)/(**5**)/(**4**) and (**3**)/(**3**) crosslinked hydrogel, the dried copolymer sample was dissolved in a 150 µL HEPES buffer (10×10^{-3} M HEPES, 100×10^{-3} M $MgCl_2$, pH 7.0) to yield a mixture containing 1.40×10^{-3} M nucleic acids in the presence of added stand (**5**). The resulting mixture was heated to 95 °C, to yield a homogenous aqueous polymer solution. The hot solution was poured into a triangle-shaped tetrafluoroethylene mold and was allowed to cool down to room temperature. After incubation for 2 h, the resulting shaped (**4**)/(**5**)/(**4**) and (**3**)/(**3**) crosslinked hydrogel was removed from the mold.

For the transitions of the (**1**)/(**2**) and (**3**)/(**3**) crosslinked hydrogel to a quasi-liquid state and its recovery to the shaped structure, the triangle-shaped structure was immersed in an HEPES buffer (10×10^{-3} M HEPES, 100×10^{-3} M $MgCl_2$, pH 5.0) for 1 h. The surrounding solution was removed to yield an amorphous, nonshaped quasi-liquid phase of the polymer. To recover the shaped hydrogel, an HEPES buffer (10×10^{-3} M HEPES, 100×10^{-3} M $MgCl_2$, pH 7.0) was added to the amorphous quasi-liquid, and the recovery of the polymer shaped structure occurred within 2 h. The surrounding solution was removed and the triangle-shaped hydrogel kept its structure for several hours with no noticeable changes, and the hydrogel retained its structure in the buffer solution for several days without structure change. It should be noted that the hydrogel was stained with Gel Red.

For the transitions of the (**4**)/(**5**)/(**4**) and (**3**)/(**3**) crosslinked hydrogel to a quasi-liquid state and its recovery to the shaped structure, the triangle-shaped structure was immersed in an HEPES buffer (10×10^{-3} M HEPES, 100×10^{-3} M $MgCl_2$, pH 10.0) for 1 h. The surrounding solution was removed to yield an amorphous, nonshaped quasi-liquid phase of the polymer. To recover the shaped hydrogel, an HEPES buffer (10×10^{-3} M HEPES, 100×10^{-3} M $MgCl_2$, pH 7.0) was added to the amorphous quasi-liquid, and the recovery of the polymer shaped structure occurred within 2 h. The surrounding solution was removed and the triangle-shaped hydrogel kept its structure for several hours with no noticeable changes, and the hydrogel retained its structure in the buffer solution for several days without structure change. It should be noted that the hydrogel was stained with SYBR Green I.

The formation of two-arrowhead-shaped hydrogel followed the procedures described in the caption of Figure 5. The stimuli-triggered transitions of the two-arrowhead-shaped hydrogels between shaped hydrogel structures and quasi-liquid states were achieved by applying the conditions mentioned above for each hydrogel, respectively.

Rheology Measurements: The in situ hydrogel formation, mechanical properties, and cross-linking kinetics were characterized by a HAAKE MARS III rheometer (Thermo Scientific). Time-sweep oscillatory tests

© 2015 WILEY-VCH Verlag GmbH & Co. KGaA, Weinheim

were performed with a 20 mm parallel-plate geometry, using 120 µL of a copolymer chains solution (resulting in a gap size of 0.25 mm), 1 min after its preparation, at a temperature of 25 °C. The linear viscoelastic region was found to be in the range of 1% strain and 1 Hz frequency.

NMR Measurements: The average molecular weight of the copolymers P_1 (Figure 1A) and P_2 (Figure 3A) was determined by diffusion-ordered NMR spectroscopy (DOSY), which relates the chemical shifts of NMR resonances of a given molecule to the translational diffusion coefficient of the species. This method turned out to be a facile method for determining average molecular weights. As shown in Figure S1 (Supporting Information), a calibration curve corresponding to the diffusion coefficients of poly(acrylic acid) of variable known molecular weights (30 000, 200 000, and 450 000) was deduced. The linear equation is $y = -0.9683x - 6.105$ ($R^2 = 0.9628$). Average molecular weights were calculated as 160 000 and 180 000 for P_1 and P_2, respectively. The NMR spectra were recorded on a Bruker DRX 400 MHz or a Bruker Ultrashield Plus 500 MHz spectrometer. The NMR spectra were referenced to residual solvent signals and recorded at 298 K. 1H NMR data are reported as follows: chemical shift in ppm on the δ scale, integration, and multiplicity (s, singlet; d, doublet; t, triplet; q, quartet; dd, doublet of doublets; bs, broad singlet; bm, broad multiplet; m, multiplet). Standard samples of 0.5 mg of commercially available poly(acrylic acid)s in 1 mL of D_2O were used for the calibration curve in the DOSY experiments.

Microscopy Measurements: SEM images were taken with Extra High Resolution Scanning Electron Microscope Magellan (TM) 400L, microscope Settings: 2 kV, 6.3 pA. Slides (Si) were first washed with distilled water followed by ethanol and acetone, and then UV/ozone cleaned using a T1O×10/OES/E UV/ozone chamber from UVOCS, Inc. (USA). Subsequently, the slides were incubated in 2% aminopropyltriethoxysilane for 30 min and heated to 110 °C for 10 min to generate an amino monolayer. A piece of hydrogel or a droplet of quasi-liquid was placed on the slide surface. Then the samples were frozen by immersing it in liquid nitrogen. The frozen samples were dried by sublimation of the formed ice under high vacuum, and the resulting surfaces were further metal-coated with Au/Pd.

Supporting Information

Supporting Information is available from the Wiley Online Library or from the author.

Acknowledgements

Y.H. and C.-H.L. contributed equally to this work. This research was supported by the NanoSensoMach ERC Advanced Grant (No. 267574) under the European Union's 7th Framework Programme (FP7/2007-2013).

Received: July 28, 2015
Revised: September 10, 2015
Published online: October 19, 2015

[1] a) A. Lendlein, S. Kelch, *Angew. Chem. Int. Ed.* **2002**, *41*, 2034; b) C. Liu, H. Qin, P. T. Mather, *J. Mater. Chem.* **2007**, *17*, 1543; c) M. Yoshida, R. Langer, A. Lendlein, J. Lahann, *J. Macromol. Sci., Polym. Rev.* **2006**, *46*, 347; d) H. Meng, G. Li, *Polymer* **2013**, *54*, 2199; e) K. K. Julich-Gruner, C. Löwenberg, A. T. Neffe, M. Behl, A. Lendlein, *Macromol. Chem. Phys.* **2013**, *214*, 527; f) R. Mohr, K. Kratz, T. Weigel, M. Lucka-Gabor, M. Moneke, A. Lendlein, *Proc. Natl. Acad. Sci. USA* **2006**, *103*, 3540; g) L. Sun, W. M. Huang, Z. Ding, Y. Zhao, C. C. Wang, H. Purnawali, C. Tang, *Mater. Des.* **2012**, *33*, 577; h) M. Bothe, T. Pretsch, *J. Mater. Chem. A* **2013**, *1*, 14491; i) I. A. Rousseau, *Polym. Eng. Sci.* **2008**, *48*, 2075; j) T. Pretsch, *Polymers* **2010**, *2*, 120.

[2] T. Miyata, N. Asami, T. Uragami, *Nature* **1999**, *399*, 766.

[3] a) A. Khaldi, J. A. Elliott, S. K. Smoukov, *J. Mater. Chem. C* **2014**, *2*, 8029; b) I. H. Paik, N. S. Goo, Y. C. Jung, J. W. Cho, *Smart Mater. Struct.* **2006**, *15*, 1476; c) Q. Ge, K. K. Westbrook, P. T. Mather, M. L. Dunn, H. Jerry Qi, *Smart Mater. Struct.* **2013**, *22*, 055009; d) S. Imai, K. Sakurai, *Precis. Eng.* **2013**, *37*, 572; e) M. Ahmad, J. Luo, M. Miraftab, *Sci. Technol. Adv. Mater.* **2012**, *13*, 015006; f) L. Sun, W. M. Huang, C. C. Wang, Z. Ding, Y. Zhao, C. Tang, X. Y. Gao, *Liq. Cryst.* **2014**, *41*, 277; g) M. Bothe, T. Pretsch, *Macromol. Chem. Phys.* **2012**, *213*, 2378.

[4] a) Y. Qiu, K. Park, *Adv. Drug Delivery Rev.* **2012**, *64*, 49; b) M. Behl, J. Zotzmann, A. Lendlein, *Adv. Polym. Sci.* **2009**, *226*, 1.

[5] a) H. Koerner, G. Price, N. A. Pearce, M. Alexander, R. A. Vaia, *Nat. Mater.* **2004**, *3*, 115; b) A. Lendlein, R. Langer, *Science* **2002**, *296*, 1673; c) J. Kunzelman, T. Chung, P. T. Mather, C. Weder, *J. Mater. Chem.* **2008**, *18*, 1082; d) M. Ecker, T. Pretsch, *RSC Adv.* **2014**, *4*, 286; e) M. Ebara, K. Uto, N. Idota, J. M. Hoffman, T. Aoyagi, *Soft Matter.* **2013**, *9*, 3074; f) T. Pretsch, M. Ecker, M. Schildhauer, M. Maskos, *J. Mater. Chem.* **2012**, *22*, 7757.

[6] a) Y. Osada, A. Matsuda, *Nature* **1995**, *376*, 219; b) W. M. Huang, C. L. Song, Y. Q. Fu, C. C. Wang, Y. Zhao, H. Purnawali, H. B. Lu, C. Tang, Z. Ding, J. L. Zhang, *Adv. Drug Delivery Rev.* **2013**, *65*, 515; c) J. L. Zhang, W. M. Huang, H. B. Lu, L. Sun, *Mater. Des.* **2014**, *53*, 1077.

[7] F. Wang, X. Liu, I. Willner, *Angew. Chem. Int. Ed.* **2015**, *54*, 1098.

[8] a) D. Liu, S. Balasubramanian, *Angew. Chem. Int. Ed.* **2003**, *42*, 5734; b) J. Sharma, R. Chhabra, H. Yan, Y. Liu, *Chem. Commun.* **2007**, 477; c) W. Wang, Y. Yang, E. Cheng, M. Zhao, H. Meng, D. Liu, D. Zhou, *Chem. Commun.* **2009**, 824; d) C. Wang, Z. Huang, Y. Lin, J. Ren, X. Qu, *Adv. Mater.* **2010**, *22*, 2792; e) J. Elbaz, S. Shimron, I. Willner, *Chem. Commun.* **2010**, *46*, 1209; f) X. Wang, J. Huang, Y. Zhou, S. Yan, X. Weng, X. Wu, M. Deng, X. Zhou, *Angew. Chem. Int. Ed.* **2010**, *49*, 5305; g) S. Shimron, N. Magen, J. Elbaz, I. Willner, *Chem. Commun.* **2011**, *47*, 8787.

[9] a) D. Monchaud, P. Yang, L. Lacroix, M. P. Teulade-Fichou, J. L. Mergny, *Angew. Chem. Int. Ed.* **2008**, *47*, 4858; b) A. Ono, S. Cao, H. Togashi, M. Tashiro, T. Fujimoto, T. Machinami, S. Oda, Y. Miyake, I. Okamoto, Y. Tanaka, *Chem. Commun.* **2008**, 4825; c) D. Han, Y. R. Kim, J. W. Oh, T. H. Kim, R. K. Mahajan, J. S. Kim, H. Kim, *Analyst* **2009**, *134*, 1857; d) T. Li, L. Shi, E. Wang, S. Dong, *Chem. Eur. J.* **2009**, *15*, 3347; e) S. Shimron, J. Elbaz, A. Henning, I. Willner, *Chem. Commun.* **2010**, *46*, 3250.

[10] a) Y. Liu, D. Sen, *J. Mol. Biol.* **2004**, *341*, 887; b) X. Liang, H. Nishioka, N. Takenaka, H. Asanuma, *ChemBioChem* **2008**, *9*, 702; c) H. Kang, H. Liu, J. A. Phillips, Z. Cao, Y. Kim, Y. Chen, Z. Yang, J. Li, W. Tan, *Nano Lett.* **2009**, *9*, 2690; d) D. Han, J. Huang, Z. Zhu, Q. Yuan, M. You, Y. Chen, W. Tan, *Chem. Commun.* **2011**, *47*, 4670; e) Y. Yang, M. Endo, K. Hidaka, H. Sugiyama, *J. Am. Chem. Soc.* **2012**, *134*, 20645; f) M. X. You, F. J. Huang, Z. Chen, R. W. Wang, W. H. Tan, *ACS Nano* **2012**, *6*, 7935; g) Y. Zou, J. Chen, Z. Zhu, L. Lu, Y. Huang, Y. Song, H. Zhang, H. Kang, C. J. Yang, *Chem. Commun.* **2013**, *49*, 8716.

[11] a) Z. G. Wang, J. Elbaz, I. Willner, *Nano Lett.* **2011**, *11*, 304; b) J. Elbaz, Z. G. Wang, R. Orbach, I. Willner, *Nano Lett.* **2009**, *9*, 4510; c) Z. G. Wang, J. Elbaz, F. Remacle, R. D. Levine, I. Willner, *Proc. Natl. Acad. Sci. USA* **2010**, *107*, 21996.

[12] K. Lund, A. J. Manzo, N. Dabby, N. Michelotti, A. Johnson-Buck, J. Nangreave, S. Taylor, R. Pei, M. N. Stojanovic, N. G. Walter, E. Winfree, H. Yan, *Nature* **2010**, *465*, 206.

[13] a) T. Liedl, H. Dietz, B. Yurke, F. Simmel, *Small* **2007**, *3*, 1688; b) C. H. Lu, X. J. Qi, R. Orbach, H. H. Yang, I. Mironi-Harpaz, D. Seliktar, I. Willner, *Nano Lett.* **2013**, *13*, 1298; c) Y. Xing,

© 2015 WILEY-VCH Verlag GmbH & Co. KGaA, Weinheim

E. Cheng, Y. Yang, P. Chen, T. Zhang, Y. Sun, Z. Yang, D. Liu, *Adv. Mater.* **2011**, *23*, 1117; d) H. Lin, Y. Zou, Y. Huang, J. Chen, W. Y. Zhang, Z. Zhuang, G. Jenkins, C. J. Yang, *Chem. Commun.* **2011**, *47*, 9312; e) W. Guo, C. H. Lu, X. J. Qi, R. Orbach, M. Fadeev, H. H. Yang, I. Willner, *Angew. Chem. Int. Ed.* **2014**, *53*, 10134; f) E. Cheng, Y. Xing, P. Chen, Y. Yang, Y. Sun, D. Zhou, L. Xu, Q. Fan, D. Liu, *Angew. Chem. Int. Ed.* **2009**, *48*, 7660; g) W. Guo, C. H. Lu, R. Orbach, F. Wang, X. J. Qi, A. Cecconello, D. Seliktar, I. Willner, *Adv. Mater.* **2015**, *27*, 73.

[14] J. Ren, Y. Hu, C. H. Lu, W. Guo, M. A. Aleman-Garcia, F. Ricci, I. Willner, *Chem. Sci.* **2015**, *6*, 4190.

[15] W. Guo, X. J. Qi, R. Orbach, C. H. Lu, L. Freage, I. Mironi-Harpaz, D. Seliktar, H. H. Yang, I. Willner, *Chem. Commun.* **2014**, *50*, 4065.

[16] B. Soontornworajit, J. Zhou, Z. Zhang, Y. Wang, *Biomacromolecules* **2010**, *11*, 2724.

[17] K. A. Joseph, N. Dave, J. Liu, *ACS Appl. Mater. Interfaces* **2011**, *3*, 733.

[18] X. He, B. Wei, Y. Mi, *Chem. Commun.* **2010**, *46*, 6308.

[19] S. Lilienthal, Z. Shpilt, F. Wang, R. Orbach, I. Willner, *ACS Appl. Mater. Interfaces* **2015**, *7*, 8923.

[20] J. Lee, S. M. Peng, D. Y. Yang, Y. H. Roh, H. Funabashi, N. Park, E. J. Rice, L. W. Chen, R. Long, M. M. Wu, D. Luo, *Nat. Nanotechnol.* **2012**, *7*, 816.

[21] a) A. Amodio, B. Zhao, A. Porchetta, A. Idili, M. Castronovo, C. Fan, F. Ricci, *J. Am. Chem. Soc.* **2014**, *136*, 16469; b) A. Idili, A. Vallee-Belisle, F. Ricci, *J. Am. Chem. Soc.* **2014**, *136*, 5836; c) A. Porchetta, A. Idili, A. Vallee-Belisle, F. Ricci, *Nano Lett.* **2015**, *15*, 4467.

© 2015 WILEY-VCH Verlag GmbH & Co. KGaA, Weinheim